An LX-10 Kinetic Model Calibrated Using Simulations of Multiple Small-Scale Thermal Safety Tests

Aaron P. Wemhoff,* William M. Howard, Alan K. Burnham, and Albert L. Nichols III

Lawrence Livermore National Laboratory, P.O. Box 808, L-227, Livermore, California 94551-9900

Received: May 12, 2008; Revised Manuscript Received: June 25, 2008

A new chemical kinetic model for the $\beta-\delta$ transition and decomposition of LX-10 (95% octahydro-1,3,5,7-tetranitro-1,3,5,7-tetrazocine, 5% Viton A binder) is presented here. This model implements aspects of previous kinetic models but calibrates the model parameters to data sets of three experiments: differential scanning calorimetry (DSC), thermogravimetric analysis (TGA), and one-dimensional time to explosion (ODTX). The calibration procedure contains three stages: one stage uses open-pan DSC and TGA to develop a base reaction for formation of heavy gases, a second stage features closed-pan DSC to ascertain the autocatalytic behavior of reactant gases attacking the solid explosive, and a final stage adjusts the rate for the breakdown of heavy reactant gases using ODTX experimental data. The resultant model presents a large improvement in the agreement between simulated DSC and TGA results and their respective experiments while maintaining the same level of agreement with ODTX, scaled thermal explosion, and laser heating explosion times when compared to previous models.

1. Existing HMX Kinetic Models

The proper characterization of explosives is vital for military and civilian applications, safe handling, and maintenance. One such explosive, octahydro-1,3,5,7-tetranitro-1,3,5,7-tetrazocine (HMX), has been well-studied in recent years because of its importance. The chemical kinetics of this explosive and its related mixtures has been examined via both cookoff experiments and computer simulations. Behrens et al.[1] provided a detailed HMX decomposition reaction framework, but determination of appropriate kinetic parameters for these reactions for the purposes of cookoff simulations is currently infeasible and impractical. Tarver and Tran established a general formulation chemical kinetics for HMX and its mixtures that follows a sequential reaction network[2] by modeling one-dimensional time to explosion (ODTX)[3,4] experiments using the chemical TOPAZ[5] thermochemical finite element code. Their HMX kinetic model framework, denoted "Tarver–Tran" in this article, is as follows in our notation:

$$\begin{aligned} &\beta \rightarrow \delta \\ &\delta \rightarrow f \\ &f \rightarrow hg \\ &hg + hg \rightarrow 2lg \end{aligned} \tag{1}$$

In the above sequential reaction framework, the first three reactions are first-order Arrhenius, whereas the final reaction is second-order Arrhenius. The characters β, δ, f, hg, and lg represent the β and δ HMX phases, solid fragments, heavy gas products, and light gas products, respectively. Table 1 provides details regarding the kinetic reaction framework, activation energies E, frequency factors A, and heats of reaction Q for this model. Note that a positive value of Q represents an endothermic reaction, and the $\beta-\delta$ transition reaction energy used in this model is approximately 26% higher than the reaction enthalpy of 33.1 kJ/kg determined experimentally by Krien et al.[6] The parameters x, R, and T represent the reactant species mass fraction, ideal gas constant, and temperature, respectively. The Tarver–Tran model provides good agreement with isothermal ODTX experimental data while maintaining a sound physical basis for the evolution of the molecular structure during decomposition. This model has also been validated on other cookoff experiments such as ramped ODTX[2] and laser ignition tests.[7]

TABLE 1: Tarver–Tran Kinetic Reactions, Parameters, and Heats of Reaction[2]

reaction	kinetic rate expression	parameter values
$\beta \rightarrow \delta$	$k = Ax_\beta \exp(-E/RT)$	$E = 202.8$ kJ/mol $\ln A/s^{-1} = 48.13$ $Q = +41.8$ kJ/kg
$\delta \rightarrow f$	$k = Ax_\delta \exp(-E/RT)$	$E = 220.5$ kJ/mol $\ln A/s^{-1} = 48.7$ $Q = +251.0$ kJ/kg
$f \rightarrow hg$	$k = Ax_f \exp(-E/RT)$	$E = 185.4$ kJ/mol $\ln A/s^{-1} = 37.8$ $Q = -556.5$ kJ/kg
$hg + hg \rightarrow 2lg$	$k = Ax_{hg}^2 \exp(-E/RT)$	$E = 142.7$ kJ/mol $\ln A/s^{-1} = 28.1$ $Q = -5594.0$ kJ/kg

Wemhoff et al.[8] recently provided an alternative chemical kinetic model for HMX using an autocatalytic bidirectional approach for the $\beta-\delta$ transition and a single-step Prout–Tompkins decomposition from the β and δ solid phases to the products. Their approach provides a general means of approximating a varying degree of autocatalysis during decomposition but does not reflect any particular molecular breakup procedure. Our calibrated version of this model, denoted "two-step" in this article, is written as the following reaction sequence:

$$\begin{aligned} &\beta \leftrightarrow \delta \\ &\beta + \delta \leftrightarrow 2\delta \\ &(\beta, \delta) \rightarrow lg \end{aligned} \tag{2}$$

where both $\beta-\delta$ transition reactions are of bidirectional type,

* To whom correspondence should be addressed. E-mail: aaron.wemhoff@villanova.edu.

10.1021/jp804190r CCC: $40.75
Published on Web 08/30/2008

$$k = Ax \exp\left(-\frac{E}{RT}\right) \sinh\left(\Lambda^* - \frac{E_e^*}{RT}\right) \quad (3)$$

and the decomposition reaction follows the extended Prout−Tompkins model,

$$k = Ax^n[1 - q(x_\beta + x_\delta)]^m \exp\left(-\frac{E}{RT}\right) \quad (4)$$

Wemhoff et al.[8] showed that the two-step model provides substantial improvement over the Tarver−Tran model in modeling the $\beta-\delta$ transition endotherm in both the Sandia instrumented thermal ignition (SITI)[9] and scaled thermal explosion (STEX)[10,11] slow cookoff experiments. In addition, the use of a Prout−Tompkins decomposition reaction provides an efficient means to calibrate a general model for a variety of explosives.[12] Levitas et al.[13] recently provided HMX decomposition kinetics that follows an approach similar to the two-step method.

2. Improvements to the Existing Models

Recent work by Nichols et al.[14] shows that STEX simulations of LX-10 (95% HMX, 5% Viton binder) using either existing kinetic model have a much larger amount of strain past the 60 h mark than in the corresponding experiment. We hypothesize that these kinetic models predict formation of product gases too early in the simulation, which in turn pressurizes the STEX cylinder causing excessive mechanical strain. This excessive early gas generation is reflected in simulations of differential scanning calorimetry (DSC) and thermogravimetric analysis (TGA)[15] experiments, as will be shown later in this article. Therefore, the goal of this study is to create an LX-10 kinetics framework that reduces gas generation during the early stages of the decomposition process while maintaining the agreement in ODTX times and simulated STEX surface temperatures at explosion in both the Tarver−Tran and two-step models.[2,8]

Aspects of both existing kinetic models were used in the development of a new kinetic model. The new model contains several sequential decomposition steps as in the Tarver−Tran model, yet the $\beta-\delta$ phase transition is described in a manner similar to the two-step model. The use of the Tarver−Tran HMX model as a framework for the LX-10 as a basis is justified, since during the decomposition process the Viton is generally inert, although recent work has suggested a minor effect on thermal decomposition.[16] Here we assume that the heats of formation used in the Traver−Tran model provide reasonable approximations to the energies of formation used in the new model. Other binders such as that in PBX-9501 may have more influence on the HMX chemical decomposition, so additional reactions may be required for those chemical mixtures.

In the $\beta-\delta$ transition, Wemhoff et al.[8] used an activation energy E and frequency factor A from Burnham et al.,[17] and the parameters Λ^* and E_e were adjusted on the basis of an assumed equilibrium constant of $K_o = 15.3$ and equilibrium temperature of 160 °C. Here, simulations of the SITI experiment were used to calibrate the values of A, E, and the equilibrium temperature. A simulation using the $\beta-\delta$ transition model of Henson and co-workers[18,19] was first applied to create a centerline endotherm for calibration, and then later simulations of pure HMX using the bidirectional reaction kinetics were applied in the calibration process. Figure 1 shows that the current approach can be brought into agreement with the Henson−Smilowitz model for an activation energy, frequency factor, and equilibrium temperature of 425.9 kJ/mol, 4.4×10^{46} s^{-1}, and 155 °C, respectively. It should be noted that this calibrated activation energy exceeds the value of approximately 209 kJ/mol estimated by previous thermochemical arguments[18,19] and other investigations suggested nucleation activation energies of 335[16] and 310 kJ/mol,[13] and thus further investigation is necessary. One possible explanation for this discrepancy is that the Henson and co-workers model uses PBX-9501, which contains an energetic binder that may affect the calibrated activation energy and frequency factor here.

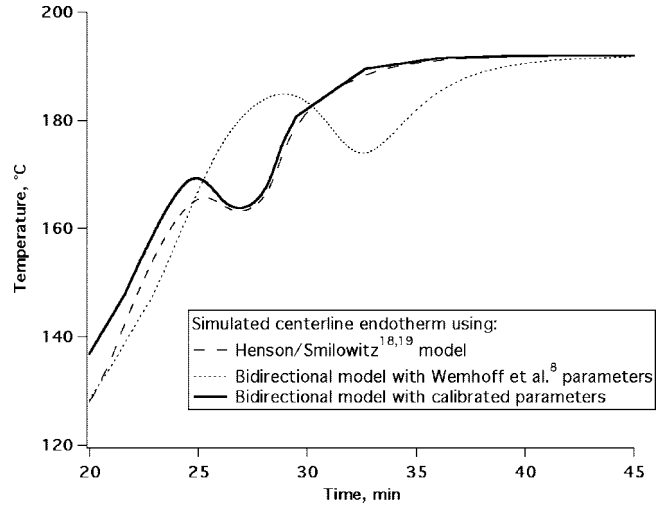

Figure 1. Simulated thermocouple readings in the SITI experiment.

TABLE 2: Reaction Networks To Be Calibrated

reaction number	reaction description	activation energy is assumed to be same for the listed Tarver−Tran reaction
R1	$\beta \leftrightarrow \delta$	N/A
R2	$\beta + \delta \leftrightarrow 2\delta$	N/A
R3	$\beta \rightarrow f$	$\delta \rightarrow f$
R4	$\delta \rightarrow f$	$\delta \rightarrow f$
R5	$f \rightarrow hg$	$f \rightarrow hg$
R6	$f + hg \rightarrow 2hg$	$f \rightarrow hg$
R7	$hg + hg \rightarrow 2lg$	$hg + hg \rightarrow 2lg$

A second modification to the Tarver−Tran model stems from the fact that experiments such as low temperature decomposition by Burnham et al.[20] demonstrate the breakdown of β-HMX below the phase transition temperature, which implies a parallel decomposition mechanism of β-HMX to solid fragments. Furthermore, the chemical equivalence between β-HMX and δ-HMX suggests that a first-order approximation to the model is to apply equivalent activation energy values in their decomposition into solid fragments.

Finally, it is anticipated that the presence of heavy gas molecules in a sealed system would attack the remaining solid HMX, which corresponds to an autocatalytic reaction. The detailed reaction network of Behrens et al. suggests the presence of autocatalysis in the HMX decomposition.[1] The Tarver−Tran model is sequential and does not include any autocatalysis, and the Prout−Tompkins model implies some limited amount of autocatalysis independent of experimental system imposed. In reality, the addition of autocatalysis represents a means to account for the confinement of the system. One reasonable approximation is to assume no presence of an autocatalytic reaction for open systems such as TGA and open pan DSC, while including a single autocatalytic reaction for sealed systems such as closed-pan DSC and ODTX.

Table 2 provides the new kinetic model to be calibrated. The approach used in this study considers the use of Tarver−Tran activation energies to be a reasonable first approximation for the various decomposition steps, while the frequency factors

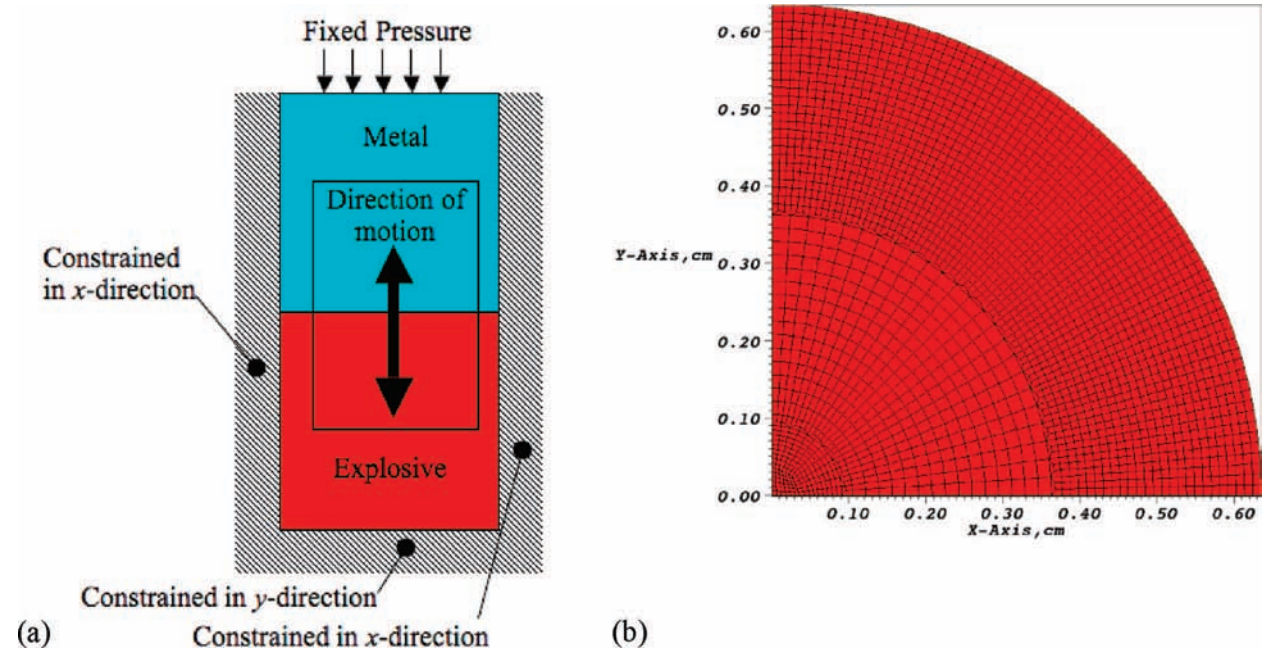

Figure 2. Schematic for DSC/TGA (a) and ODTX (b) simulation. Both elements of DSC/TGA mesh contain an initial length of 1 cm on all four sides, and units of the ODTX mesh are in centimeters.

were adjusted to calibrate the model on the basis of the aforementioned changes. In addition, the material models used in this study were updated since the earlier studies were performed, and this study uses a hydrodynamic code that allows for inclusion of pressure expansion work effects in the material energy, unlike the chemical TOPAZ code used in the Tarver−Tran calibration. Finally, this study combines results from multiple small-scale thermal cookoff experiments for calibration of the kinetics unlike the earlier studies, and this point is discussed further in the next section.

3. Experimental Models

Three systems (DSC, TGA, and ODTX) were modeled using the LLNL Arbitrary Lagrangian-Eulerian hydrodynamic code ALE3D.[21] The models for these systems are now described in detail.

A. DSC and TGA. DSC experiments apply a fixed temperature ramp on a small sample of explosive, which allows for measurements of heat gain and loss into the pan due to chemical reactions. The DSC models use implicit hydrodynamics since the amount of volumetric expansion is not negligible and has an effect on the system internal energy. In general, this system contains weak material (defined as the shear modulus being small compared to bulk modulus), especially after gas formation. The only currently feasible way to model such a system implicitly with ALE3D's loosely coupled formulation is to limit the system to a single degree of freedom. Figure 2a shows the two-dimensional, two-zone plane strain piston−cylinder arrangement used to approximate the DSC experiment. The temperatures of all nodes in the system are ramped at a desired rate, and a fixed pressure (15 psia [103 kPa] for open-pan, 1000 psia [6.9 MPa] for closed-pan) is applied on the top of the metal piston. All explosive material exists in a single element in the interior of the piston. The sides and bottom of the piston−cylinder arrangement are constrained in the outward direction. The material used here is LX-10 to match experimental data.

TGA applies a fixed temperature or ramp rate to a small amount of explosive for the purposes of measuring mass loss. The model for TGA was the same as that for DSC with the exception that the mesh was constrained throughout, allowing for an explicit simulation with mass scaling. The explicit formulation was required because the implicit mechanics solver fails to converge in the isothermal cases because of the sudden change in material temperature by the applied discontinuous temperature boundary condition. This problem could potentially be mitigated in the future by initially using an explicit formulation to handle this phenomenon and then transitioning to the standard implicit formulation. In addition, the use of explicit mechanics greatly reduces required simulation time compared to implicit mechanics. The mass loss was approximated as that calculated by the formation of heavy gas products in the system (or light gases for the two-step model). Pure HMX was used for the calibration in this model to match experiment.

B. ODTX. ODTX experiments feature a fixed external boundary temperature applied by an external anvil onto a pressed explosive sphere. The ODTX computational model is a two-dimensional, axisymmetric quarter sphere of LX-10 with diameter 0.5 in. (1.27 cm), corresponding to the experiment. These simulations were performed using explicit hydrodynamics with mass scaling in the same manner as the TGA model. The outer nodes of the sphere are held to the desired fixed temperature for the run. It was assumed that an "explosion time" occurred under one of three conditions: the local LX-10 temperature rise exceeded 10^9 K/s, the maximum zonal temperature exceeded 1000 K, or the amount of final products formed exceeded 5% of the overall system mass in any zone. Figure 2b provides the mesh used in the ODTX simulations.

C. Material Properties. In this study, we apply energies of formation of +41.8 and +292.9 kJ/kg for δ-HMX and solid fragments per Tarver and Tran[2] when implementing both kinetic models, and we use tabulated data sets for estimation of the energies of formation for the heavy and light gases. Here, we apply a zero energy of formation for β-HMX. ALE3D calculates the energy due to reaction at a given time step by multiplying the conversion mass fraction by the reduction in energy of

TABLE 3: Material Properties for Solid LX-10 Components

material	β-HMX	δ-HMX	HMX fragments	Viton
initial mass fraction, %	95	0	0	5
reference density (ρ_0), g/cc	1.865	1.755	1.755	1.865
energy of formation, kJ/kg	0.0	+41.8	+292.9	0.0
bulk modulus (K_b), GPa	13.5	13.5	13.5	13.5
K_1, GPa	81.9	80.6	80.6	81.9
γ	1.009	1.077	1.077	1.009
shear modulus, GPa	4.2	4.2	4.2	4.2
yield strength, MPa	2.1	2.1	2.1	2.1

formation as the reactant transitions into a product, but does not consider the reaction enthalpy. The solid components use the general polynomial equation of state

$$P = K_b\mu + K_1\mu^2 + \gamma\rho c_v(T - T_0) \quad (5)$$

where P is pressure, K_b is the bulk modulus, ρ is mass density, c_v is the constant volume specific heat, K_1 and γ are equation of state coefficients, and

$$\mu = \frac{\rho}{\rho_0} - 1 \quad (6)$$

The reference values of state variables P, ρ, and T are denoted by the subscript 0. The values of K_b, K_1, and γ were taken by matching shock Hugoniot, isothermal compression, and thermal expansion data from reference guides.[22,23] Values of temperature-dependent heat capacity and thermal conductivity for the solid species matched those of Tarver and Tran.[2] Table 3 provides values of the material properties used in each of the LX-10 solid species. All solid materials were assumed to contain the same shear modulus and yield strength.

We used the thermochemical code Cheetah[24] to model the equations of state for the heavy and light gases formed during HMX decomposition. This code was developed during the past decade at the LLNL Energetic Materials Center and is widely used for the study of high explosive and explosive formulations. Cheetah solves thermodynamic equations between product species to find chemical equilibrium, and it can calculate multispecies and multiphase chemical equilibrium. Thermodynamics equilibrium is found by balancing chemical potentials. For the "light" product gas equation of state, we assumed that HMX decomposes to its full chemical equilibrium products as a function of temperature and density. For the "heavy" product equation of state, we assumed that HMX can decompose only in stoichiometric proportions to the radicals N_2O and CH_2O; that is,

$$C_4H_8N_8O_8 \rightarrow 4CH_2O + 4N_2O \quad (7)$$

Figures 3 and 4 provide isotherms for these two cases. For the equation of state, we use a statistical-based calculation based on exp-6 (Buckingham potential)[25] fluids that are calibrated up to high (a few megabars) pressures and high temperatures (approximately 20 000 K). For the calibration, we use shock Hugoniot data to a few megabars, as well as sound speed and compression data to determine the potential parameters. The temperature-dependent heat capacities are valid to 20 000 K. The heat capacity and sound velocity information for these mixtures was then applied via Bridgmann's relation for liquids[26] to obtain the temperature-dependent thermal conductivity.

4. Calibration Methodology

The general approach used here was to build the reaction network in stages by approximating the presence of certain

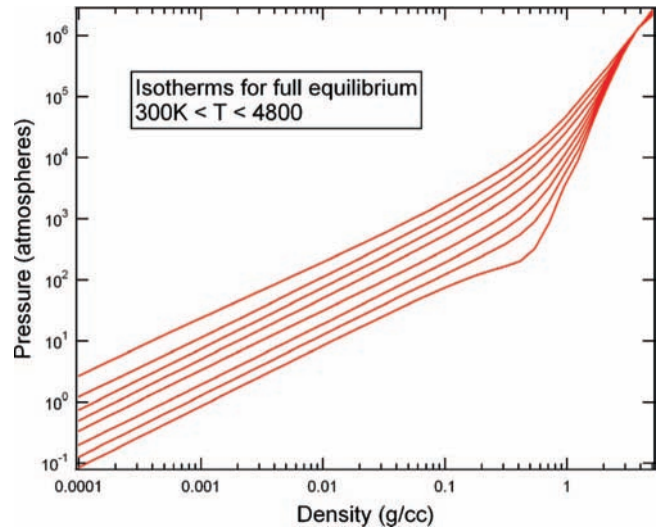

Figure 3. Calculated isotherms for the case of assuming full chemical equilibrium ("light" gas approximation).

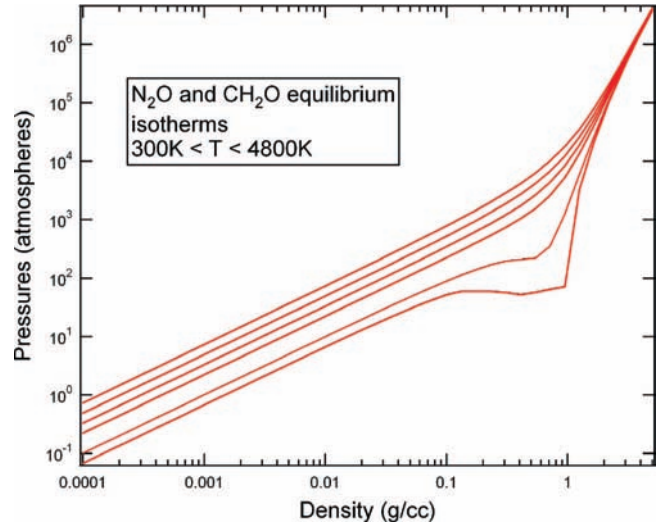

Figure 4. Calculated isotherms for the case of assuming only N_2O and CH_2O equilibrium ("heavy" gas approximation).

reactions for a given experiment. The optimization in each stage was based on the minimization of an overall figure of merit (FOM) calculated by comparing modeled and experimental results. In general, the FOM is calculated as

$$\mathrm{FOM} = \sum_{i=1}^{N_{DSC}} (F_{DSC})_i^2 + \sum_{i=1}^{N_{TGA}} (F_{TGA})_i^2 + \sum_{i=1}^{N_{ODTX}} (F_{ODTX})_i^2 \quad (8)$$

where the number of DSC, TGA, and ODTX experiments is N_{DSC}, N_{TGA}, and N_{ODTX}, respectively. The value of F_i is the percentage error of model run i when compared to the corresponding experimental data.

Calibration was performed by applying a steepest descents/1-d bisection algorithm applied as a wrapper script over ALE3D simulations of the model experiments. For a series of samples, the gradient of the FOM first determined the direction of steepest descent, and then a series of 15 bisections were used to determine the minimum FOM along the steepest descent line between the starting point and the edge of the parameter domain.

The goal of this calibration process is to obtain the parameters for reactions R3 through R7 in the network shown in Table 2. Since the optimization of five frequency factors is a difficult task for any calibration procedure, the approach here is to

TABLE 4: Calibration Stages and Reaction Treatment

reaction number	reaction description	treatment for each calibration stage[a] stage 1: TGA and open DSC	stage 2: closed DSC	stage 3: ODTX
R1	$\beta \leftrightarrow \delta$	A	A	A
R2	$\beta + \delta \leftrightarrow 2\delta$	A	A	A
R3	$\beta \rightarrow f$	C	A	A
R4	$\delta \rightarrow f$	C	A	A
R5	$f \rightarrow hg$	C	A	A
R6	$f + hg \rightarrow 2hg$	I	C	A
R7	$hg + hg \rightarrow 2lg$	I	I	C

[a] Treatment options: Apply without changing (A), Calibrate (C), and Ignore (I).

provide approximations in the systems that allow us to ignore some reactions. For example, open systems would not contain a large amount of autocatalysis in gas formation because the gases escape the system, so autocatalyic reactions may be ignored in TGA and open-pan DSC. In addition, constant volume explosions as in ODTX experiments produce pressures several orders of magnitude beyond the range of sealed DSC enclosures, and the final gas-phase reaction may be ignored for sealed DSC if the reaction is assumed to require pressures beyond the closed-pan seal rating of approximately 1000 psi (6.9 MPa). Table 4 describes which reactions are applied, calibrated, and ignored in each of the three stages of calibration, which reduces the calibration requirements to 1−3 parameters per stage.

A. TGA and Open-Pan DSC. In the first stage, the ambient pressure experiments (TGA and open-pan DSC) were used to allow for calibration of reactions R3 through R5. Reactions R6 and R7 were not applied in this system since it is assumed that the gases escape the immediate vicinity of the experiment and therefore do not react. The final gas-phase reaction of the Tarver−Tran model was ignored for this reason as well. The $\beta-\delta$ phase transition kinetics were implemented but not altered. The varied parameters were the natural logarithm of the frequency factors for reactions R3, R4, and R5, and the ranges for $\ln A_3/s^{-1}$, $\ln A_4/s^{-1}$ and $\ln A_5/s^{-1}$ were 28.8−63.8, 28.8−63.8, and 23.8−53.8, respectively.

Burnham and co-workers[20,27] provide the experimental TGA and open-pan DSC data for calibration. These data include 50% decomposition data for isothermal runs at 250 °C (25 min) and 230 °C (120 min), and 10% decomposition data at 120 °C (5×10^6 min), where the latter is taken from N_2O formation measurements and is important, as it provides a low-temperature constraint for the decomposition process. Ramped TGA data used were 50% decomposition at 255 and 230 °C for ramp rates of 0.9 and 1.8 °C/min, respectively. Three open-pan DSC data were used: external peak energy release at 229, 245, and 261 °C for applied ramp rates of 0.1, 0.35, and 1.0 °C/min, respectively.

B. Closed-Pan DSC. The second experiment used for calibration was closed-pan DSC. The confinement of the system has a known effect on external temperatures at which peak decomposition occurs. Previous work by Burnham and co-workers,[15,20,27] Lee et al.,[28] and Piermarini et al.[29] suggests a pressure dependence on HMX decomposition. Here, we approximated the effect of confinement by the introduction of the autocatalytic reaction R6, although other methods could potentially be used, such as the multiplication of reaction rate by system pressure to a known exponent. The final reaction in the Tarver−Tran model was also ignored in closed-pan DSC models for comparison with the new model.

TABLE 5: Calibrated Kinetic Parameters from This Study

reaction	kinetic rate expression	parameter values[a]
$\beta \leftrightarrow \delta$	$k = Ax_\beta \exp(-E/RT)$ $\sinh[\Lambda^* - (E_e^*/RT)]$	$\boldsymbol{E = 425.9}$ **kJ/mol**
		$\boldsymbol{\ln A/s^{-1} = 107.4}$
		$\boldsymbol{E_e^* = 9.71}$ **kJ/mol**
		$\Lambda^* = 2.728$
$\beta + \delta \leftrightarrow 2\delta$	$k = Ax_\beta x_\delta \exp(-E/RT)$ $\sinh[\Lambda^* - (E_e^*/RT)]$	$\boldsymbol{E = 113.0}$ **kJ/mol**
		$\boldsymbol{\ln A/s^{-1} = 29.5}$
		$\boldsymbol{E_e^* = 9.71}$ **kJ/mol**
		$\Lambda^* = 2.728$
$\beta \rightarrow f$	$k = Ax_\beta \exp(-E/RT)$	$E = 220.5$ kJ/mol
		$\boldsymbol{\ln A/s^{-1} = 50.05}$
$\delta \rightarrow f$	$k = Ax_\delta \exp(-E/RT)$	$E = 220.5$ kJ/mol
		$\boldsymbol{\ln A/s^{-1} = 50.11}$
$f \rightarrow hg$	$k = Ax_f \exp(-E/RT)$	$E = 185.4$ kJ/mol
		$\boldsymbol{\ln A/s^{-1} = 35.07}$
$f + hg \rightarrow 2hg$	$k = Ax_f x_{hg} \exp(-E/RT)$	$E = 185.4$ kJ/mol
		$\boldsymbol{\ln A/s^{-1} = 38.89}$
$hg + hg \rightarrow 2lg$	$k = Ax_{hg}^2 \exp(-E/RT)$	$E = 142.7$ kJ/mol
		$\boldsymbol{\ln A/s^{-1} = 27.57}$

[a] Calibrated parameters in this study are in bold.

The confined DSC does not appear to allow full decomposition of the heavy gas into light gas (R7). Experiments of sealed DSC show some energy output in the system, which suggests partial decomposition, although a quantitative amount is infeasible because of the presence of punctures and failure of the DSC seal. Therefore, we choose to ignore the final reaction step for two reasons: first, it greatly simplifies the calibration of R6, and second, it is assumed that partial decomposition in R7 would not greatly affect the time of peak energy release greatly beyond the uncertainty of the experimental data. The only changed parameter was $\ln A_6/s^{-1}$ with a range between 23.8 and 53.8. Closed-pan experimental data used for calibration were for a peak energy release of 217, 235, and 250 °C for ramp rates of 0.1, 0.35, and 1.0 °C/min, respectively.[20]

C. ODTX. The final calibration step features ODTX simulations of LX-10 at nine temperatures ranging from 201 to 293 °C. These simulations contain all of the reactions due to the high confinement of the system. Although the actual confining pressure is unknown, it is anticipated to be 100−200 MPa, which is much higher than that in closed-pan DSC and justifies the differentiation of the reaction networks in the two experiments. The parameter $\ln A_7/s^{-1}$ contained a range of 18.8−43.8 for this calibration.

5. Results

Table 5 provides the final kinetic parameters for the model in this study using the new model. The Prout−Tompkins model was also recalibrated to ODTX data for the updated material models per the approach mentioned by Wemhoff et al.,[8] and the model parameters are shown in Table 6. Tables 7, 8, and 9 and Figure 5 show that the simulated data by the new kinetic model compare well with experimental data. Also shown for comparison are simulated results using the Tarver−Tran model and the calibrated Prout−Tompkins model, which do not contain the same agreement with experimental DSC and TGA data as the new model. The average error of the TGA results is 0.02% for the new model but is 54% for the Tarver−Tran model. The average error is 32% for the Prout−Tompkins model where simulated values are available, and the required 10% decomposition was not reached for the isothermal TGA run at 120 °C. Similarly, the average error for the DSC results for the new,

TABLE 6: Calibrated Two-Step Model Kinetic Parameters for Comparison to the New Kinetic Model

reaction	kinetic rate expression	parameter values[a]
$\beta \leftrightarrow \delta$	$k = Ax_\beta \exp(-E/RT)$ $\sinh[\Lambda^* - (E_e^*/RT)]$	$\mathbf{E = 425.9 kJ/mol}$ $\mathbf{\ln A/s^{-1} = 107.4}$ $\mathbf{E_e^* = 9.71\ kJ/mol}$ $\Lambda^* = 2.728$
$\beta + \delta \leftrightarrow 2\delta$	$k = Ax_\beta x_\delta \exp(-E/RT)$ $\sinh[\Lambda^* - (E_e^*/RT)]$	$\mathbf{E = 113.0\ kJ/mol}$ $\mathbf{\ln A/s^{-1} = 29.5}$ $\mathbf{E_e^* = 9.71\ kJ/mol}$ $\Lambda^* = 2.728$
$(\beta,\delta) \rightarrow lg$	$k = Ax_{(\beta,\delta)}^n[1 - q(x_\beta + x_\delta)]^m$ $\exp(-E/RT)$	$\mathbf{E = 227.2\ kJ/mol}$ $\mathbf{\ln A/s^{-1} = 48.70}$ $\mathbf{n = m = 1}$ $\mathbf{p = -\log_{10}(1 - q) = 9}$

[a] Calibrated parameters in this study are in bold.

TABLE 7: Comparison of Isothermal TGA Simulation Results Using Kinetic Models from This Study, Tarver and Tran,[2] and Calibrated Prout−Tompkins to Experimental Data

		simulation target decomposition time (min)		
isothermal temp (°C)	experiment target decomposition time[a] (min)	Tarver−Tran model	Prout−Tompkins model	calibrated model in this study
250	25	3.15	8.47	23.6
230	120	10.37	50.49	121.7
120	5×10^6	1.36×10^6	N/A[b]	5.02×10^6

[a] Target decomposition mass fraction is 10% for the isothermal experiment at 120 °C and 50% for all other experiments. [b] 10% decomposition was never achieved when the Prout−Tompkins model was applied in the 120 °C isothermal case.

TABLE 8: Comparison of Ramped TGA Simulation Results Using Kinetic Models from This Study, Tarver and Tran,[2] and Calibrated Prout−Tompkins to Experimental Data

		simulation target decomposition temp (°C)		
ramp rate (°C/min)	experiment target decomposition temp (°C)	Tarver−Tran model	Prout−Tompkins model	calibrated model in this study
0.9	255	227	244	256
0.18	230	211	230	238

Tarver−Tran, and Prout−Tompkins models are 1.1, 8.8, and 5.6%, respectively. Note that the Tarver−Tran and Prout−Tompkins models do not allow for a large amount of distinction between open and sealed DSC experiments because of the lack of an additional autocatalytic reaction to distinguish between the two systems. It should be noted that Burnham et al.[27] shows good agreement with DSC and ODTX data by applying a pressure dependence of $P^{0.3}$ to the base Prout−Tompkins rate. The error in ODTX data is 30, 33, and 58% for the new, Tarver−Tran, and Prout−Tompkins models, respectively. These results show that the new kinetic model maintains the good agreement of the Tarver−Tran model with ODTX data while improving the accuracy of simulated results with both TGA and DSC experiments, and both multistep models provide better ODTX agreement than using the Prout−Tompkins approach without a pressure exponent.

Two validation tests were performed using the new model. First, simple one-dimensional LX-10 STEX simulations featuring a fixed 1×50 mesh and mass scaling were performed using these models to predict times to explosion. The calculated surface temperatures at explosion for the calibrated multistep model and Tarver−Tran models are 182.0 and 179.1 °C, respectively, which compare well with the experimental value of 188 °C for confinement at 200 MPa.[11] The new model was also applied in a more complex STEX model to estimate strain values when compared to the existing kinetic model results shown in Figure 1, and the new model shows improved agreement with experimental strain results.[14]

TABLE 9: Comparison of DSC Simulation Results Using Kinetic Models from This Study, Tarver and Tran,[2] and Calibrated Prout−Tompkins to Experimental Data

			simulated temp at peak heat release (°C)		
ramp rate (°C/min)	open/sealed	expt temp at peak heat release (°C)	Tarver−Tran model	Prout−Tompkins	this study
0.10	open	229	206.6	215.1	234.6
0.35	open	245	218.9	225.9	248.9
1.00	open	261	230.0	235.3	261.4
0.10	sealed	217	206.5	215.2	220.8
0.35	sealed	235	218.9	225.9	234.2
1.00	sealed	250	230.0	235.4	246.1

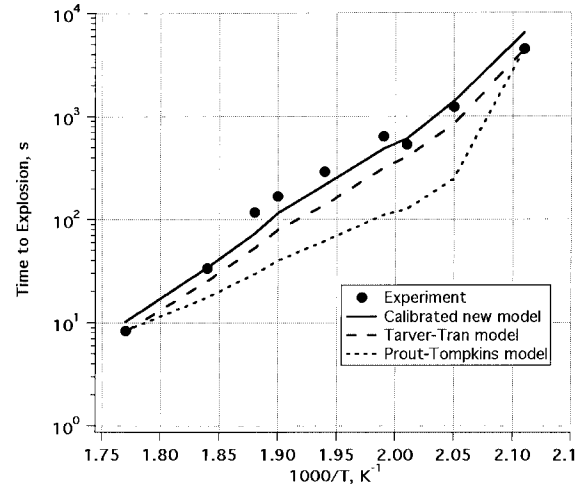

Figure 5. Comparison of experimental and simulated ODTX times, including the effects of applying implicit simulations and added air into the model and by refining the mesh by an order of magnitude. No explosion was observed for the fine mesh simulation at $1000/T = 2.11$ K^{-1}.

A second validation test involves modeling of systems with high energy fluxes and corresponding short explosion times. Henson et al.[30] provides cookoff data for HMX-based explosives in an Arrhenius-style comparative plot that spans time magnitudes from 10^{-10} to 10^5 s and corresponding surface temperatures of 2000 to 450 K. Tarver[7] modeled the cookoff ignition times for experiments by Ali et al.[31] featuring the heating of HMX and TATB by laser pulses. In general, the HMX Tarver−Tran model followed the corresponding experimental data within an order of magnitude, and the differences were attributed to melting and subsequent faster liquid-phase decomposition kinetics. Here, we apply the same methodology to both the Tarver−Tran and calibrated new models. Figure 6 shows that the calibrated model provides better agreement to experimental data when compared to the Tarver−Tran model. Furthermore, a comparison of the surface temperature at explosion versus time for these laser irradiation models shows an order-of-magnitude agreement with the empirical plot.

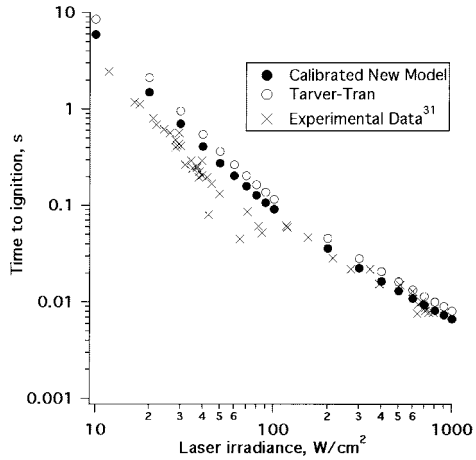

Figure 6. Comparison of experimental and simulated times to ignition for the laser experiment, where simulations used either the Tarver−Tran or calibrated new models.

6. Conclusions

The methodology used in this study provides a means for calibration of kinetic parameters in a relatively straightforward fashion. The implementation of an autocatalytic heavy gas formation mechanism delays the gas formation to better match TGA and DSC data while preserving ODTX agreement.

Areas for improvement of this kinetic model are still available. The assumptions used in applying open-pan versus sealed-pan DSC need to be explored with more detailed simulations. In addition, the applied nodal constraints in ODTX simulations are not completely reasonable since the simulated pressures of the HE in many cases exceed the seal rating of about 1 kbar, which justifies why in many cases the ODTX apparatus undergoes a pressure burst rather than thermal ignition. Also, the DSC and TGA experimental models were greatly simplified here, and more detailed simulations in the future may allow for better calibration mechanisms. In addition, the constraint of applying existing activation energies limits the ability for the kinetics to converge, and therefore allowing for the adjustment of the activation energies may provide better agreement. Finally, an appropriate pressure-dependent $\beta-\delta$ reaction mechanism was attempted here but showed a large effect on the low-temperature ODTX times, and the cause of this problem requires further investigation.

Acknowledgment. We gratefully acknowledge the effort by Matt McClelland and Jack Yoh in obtaining the material models, Rich Becker for the development of implicit hydrodynamics in ALE3D, Craig Tarver for his guidance on the kinetic models for this project, and Jaroslaw Knap for his effort in modeling the strain response of the STEX experiment. This work was performed under the auspices of the U.S. Department of Energy by Lawrence Livermore National Laboratory under Contract DE-AC52-07NA27344.

References and Notes

(1) Behrens, R. B., Jr.; Hobbs, M. L.; Margolis, S. B. A Zero-Dimensional Model of Experimental Thermal Decomposition of Cyclic Nitramines. *Proceedings of the 11th International Symposium on Detonation*, Snowmass Village, CO, Aug 31−Sept 4, 1998; U.S. Office of Naval Research: Arlington, VA, 1998; p 533.

(2) Tarver, C. M.; Tran, T. D. *Combust. Flame* **2004**, *137*, 50.

(3) Catalano, E.; Ornellas, D. L.; Wrenn, E.; Lee, E. L.; Walton, J.; McGuire, R. R. Thermal Decomposition of Trinitrotoluene (TNT) with a New One-Dimensional Time-to-Explosion (ODTX) Apparatus. *Proceedings of the 6th International Symposium on Detonation*, Karlsruhe, Germany, July 3−6, 2001; U.S. Office of Naval Research: Arlington, VA, 1976; p 214.

(4) Tran, T. D.; Simpson, L. R.; Maienschein, J.; Tarver, C. *32nd International Annual Conference of Fraunhofer Institut fur Chemische Technologie (ICT)*; DWS Werbeagentur: Karlsruhe, Germany, 2001; p 25.

(5) Nichols, A. L.; Westerberg, K. W. *Numer. Heat Transfer, Part B* **1993**, *24*, 489.

(6) Krien, G.; Licht, H. H.; Zierath, J. *Thermochim. Acta* **1973**, *6*, 465.

(7) Tarver, C. M. *J. Energ. Mater.* **2004**, *22*, 93.

(8) Wemhoff, A. P.; Burnham, A. K.; Nichols, A. L. *J. Phys. Chem. A* **2007**, *111*, 1575.

(9) Kaneshige, M. J.; Renlund, A. M.; Schmitt, R. G.; Erikson, W. W. Cook-off Experiments for Model Validation at Sandia National Laboratories. *Proceedings of the 12th International Symposium on Detonation*, San Diego, CA, Aug 11−16, 2002; U.S. Office of Naval Research: Arlington, VA, 2002; p 821.

(10) Wardell, J.; Maienschein, J. The Scaled Thermal Explosion Experiment. *Proceedings of the 12th International Symposium on Detonation*, San Diego, CA, Aug 11−16, 2002; U.S. Office of Naval Research: Arlington, VA, 2002; p 384.

(11) Maienschein, J. L.; DeHaven, M. R.; Sykora, G. B.; Black, C. K.; Wardell, J. F.; McClelland, M. A.; Strand, O. T.; Whitworth, T. L.; Martinez, C. Thermal Explosion Violence for Several Explosives−Measurements and Interpretation. *Proceedings of the 13th International Symposium on Detonation*, Norfolk, VA, July 23−28, 2006; U.S. Office of Naval Research: Arlington, VA, 2006; paper IDS097.

(12) Wemhoff, A. P.; Burnham, A. K.; Nichols, A. L.; Knap, J. *2007 Proceedings of the ASME/JSME Thermal Engineering and Summer Heat Transfer Conference*, Vancouver, BC, Canada, 2007; American Society of Mechanical Engineers: New York, July 8–12, 2007; paper HT2007-32279.

(13) Levitas, V. I.; Henson, B. F.; Smilowitz, L. B.; Zerkle, D. K.; Asay, B. W. *J. Appl. Phys.* **2007**, *102*, 113520.

(14) Nichols, A. L.; Wemhoff, A. P.; Knap, J.; Howard, W. M.; Becker, R. C. To be submitted for publication.

(15) Burnham, A. K.; Weese, R. K. *Thermal Decomposition Kinetics of HMX*; Report UCRL-TR-204262 Rev 1; Lawrence Livermore National Laboratory: Livermore, CA, 2004.

(16) Tarver, C. M.; Koerner, J. G. *J. Energ. Mater.* **2008**, *26*, 1.

(17) Burnham, A. K.; Weese, R. K.; Weeks, B. L. *J. Phys. Chem. B* **2004**, *108*, 19432.

(18) Henson, B. F.; Smilowitz, L.; Asay, B. W.; Dickson, P. M. *J. Chem. Phys.* **2002**, *117*, 3780.

(19) Smilowitz, L.; Henson, B. F.; Asay, B. W.; Dickson, P. M. *J. Chem. Phys.* **2002**, *117*, 3789.

(20) Burnham, A. K.; Weese, R. K.; Andrzejewski, W. J. *Kinetics of HMX and CP Decomposition and Their Extrapolation for Lifetime Assessment*. Presented at the 36th Annual Conference of ICT and 32nd International Pyrotechnics Seminar, Karlsrue, Germany, June 28−July 1, 2005; poster 153.

(21) Nichols, A. L. *Users Manual for ALE 3D, an Arbitrary Lagrange/Eulerian 3D Code System*; Report UCRL-MA-152204-Rev-6; Lawrence Livermore National Laboratory: Livermore, CA, 2007.

(22) Owens, C. *LLNL Explosives Reference Guide*; Report UCRL-WEB-236503; Lawrence Livermore National Laboratory: Livermore, CA, 2007.

(23) Hall, T. N.; Holden, J. R. *Navy Explosives Handbook*; Report NSWC MP88-116; Naval Surface Warfare Center: Dahlgren, VA, 1988.

(24) Fried, L. E.; Howard, W. M.; Souers, P. C. *Cheetah 3.0 User's Manual*; Report UCRL-MA-117541-Rev-6; Lawrence Livermore National Laboratory: Livermore, CA, 2000.

(25) Fried, L. E.; Howard, W. M. *J. Chem. Phys.* **1998**, *109*, 7338.

(26) Bird, R. B.; Stewart, W. E.; Lightfoot, E. N. *Transport Phenomena*; Wiley: New York, 1960.

(27) Burnham, A. K.; Weese, R. K.; Wemhoff, A. P.; Maienschein, J. L. *J. Therm. Anal. Calorim.* **2007**, *89*, 407.

(28) Lee, E. L.; Sanborn, R. H.; Stromberg, H. D. Thermal Decomposition of High Explosives at Static Pressure 10−50 Kilobars. *Proceedings of the 5th International Symposium on Detonation*, Pasadena, CA, Aug 18−21, 1970; U.S. Office of Naval Research: Arlington, VA, 1970; p 331.

(29) Piermarini, G. J.; Block, S.; Miller, P. J. *J. Phys. Chem.* **1987**, *91*, 3872.

(30) Henson, B. F.; Smilowitz, L.; Asay, B. W.; Sandstrom, M. M.; Romero, J. J. An Ignition Law for PBX 9501 from Thermal Explosion to Detonation. *Proceedings of the 13th International Symposium on Detonation*, Norfolk, VA, July 23−28, 2006; U.S. Office of Naval Research: Arlington, VA, 2006; paper IDS061, p 61.

(31) Ali, A. N.; Son, S. F.; Asay, B. W.; DeCroix, M. E.; Brewster, M. Q. *Combust. Sci. Technol.* **2003**, *175*, 1551.

JP804190R